



Privacy Preservation in MIMO-OFDM Localization Systems: A Beamforming Approach

Downloaded from: <https://research.chalmers.se>, 2026-03-15 02:46 UTC

Citation for the original published paper (version of record):

Zhang, Y., Chen, H., Keskin, M. et al (2025). Privacy Preservation in MIMO-OFDM Localization Systems: A Beamforming Approach. IEEE Wireless Communications Letters, 14(7): 1979-1983.
<http://dx.doi.org/10.1109/LWC.2025.3560219>

N.B. When citing this work, cite the original published paper.

© 2025 IEEE. Personal use of this material is permitted. Permission from IEEE must be obtained for all other uses, in any current or future media, including reprinting/republishing this material for advertising or promotional purposes, or reuse of any copyrighted component of this work in other works.

Privacy Preservation in MIMO-OFDM Localization Systems: A Beamforming Approach

Yuchen Zhang¹, Hui Chen¹, *Member, IEEE*, Musa Furkan Keskin², *Member, IEEE*, Alireza Pourafzal, Pinjun Zheng³, *Associate Member, IEEE*, Henk Wymeersch⁴, *Fellow, IEEE*, and Tareq Y. Al-Naffouri⁵, *Fellow, IEEE*

Abstract—We investigate an uplink MIMO-OFDM localization scenario where a legitimate base station (BS) aims to localize a user equipment (UE) using pilot signals transmitted by the UE, while an unauthorized BS attempts to localize the UE by eavesdropping on these pilots, posing a risk to the UE’s location privacy. To enhance legitimate localization performance while protecting the UE’s privacy, we formulate an optimization problem regarding the beamformers at the UE, aiming to minimize the Cramér-Rao bound (CRB) for legitimate localization while constraining the CRB for unauthorized localization above a threshold. A penalty dual decomposition optimization framework is employed to solve the problem, leading to a novel beamforming approach for location privacy preservation. Numerical results confirm the effectiveness of the proposed approach and demonstrate its superiority over existing benchmarks.

Index Terms—Radio localization, location privacy, Cramér-Rao bound, beamforming.

I. INTRODUCTION

LOCATION information is becoming increasingly vital, enabling a wide range of applications such as digital twins, autonomous driving, and more[1]. Although global navigation satellite systems have been widely used, they often fall short in environments with poor satellite visibility, leading to the rise of radio localization through 5G/6G cellular networks to provide seamless localization services[1], [2]. However, location data can reveal highly sensitive information, such as personal activities, raising significant privacy concerns. The inherent openness of wireless propagation leaks location information at unauthorized nodes, creating privacy threats and

highlighting the need for advanced methods to safeguard users’ location data in these evolving systems.

Physical layer security, which aims to protect communication from eavesdropping, has been widely studied [3]. However, in scenarios where location privacy preservation is crucial, such as in Internet-of-Things localization applications [4], the sole focus on communication security may not align with the primary objectives. In [5], it is shown that attackers could exploit the chosen precoder to localize users based on the location of base station (BS), suggesting that random selection among precoders that ensure high transmission rates could be an effective countermeasure. Additionally, techniques such as pilot signal modification have been proposed to prevent unauthorized localization [6], [7], [8]. However, this approach might not be practical, as standardized systems require all users to utilize predefined pilots.

Multi-antenna beamforming technologies have been widely adopted to enhance secure communication by flexibly reconfiguring the spatial distribution of signal power. While extensive research has focused on securing communication information through beamforming [3], [9], its role in preserving location privacy has received comparatively less attention. In [10] and [11], beamforming schemes are proposed that enable the user equipment (UE) to communicate securely with the BS without disclosing its location. However, these approaches often 1) struggle to balance legitimate localization with location privacy protection, and 2) do not provide a direct metric such as the Cramér-Rao bound (CRB) for location privacy, relying on metrics like signal-to-noise ratio. The challenge of optimizing beamforming to enhance legitimate localization performance while quantitatively safeguarding location privacy has received limited attention.

In this letter, we investigate a multi-input-multi-output (MIMO)-orthogonal frequency division multiplexing (OFDM) uplink localization scenario, where a legitimate BS (Bob) aims to localize a UE (Alice) based on the received pilot signals. However, these uplink pilots are also intercepted by an unauthorized BS (Eve), leading to the risk of Alice’s location information being leaked. The key contributions are summarized as follows: (i) We formulate an optimization problem to provide a reliable localization of Alice for Bob, while quantitatively protecting Alice’s location privacy from Eve. The problem minimizes the CRB of legitimate localization, subject to constraining the CRB of the unauthorized localization above a predefined threshold. (ii) We address the non-convex problem using matrix lifting and the penalty dual decomposition (PDD) optimization framework, introducing

Received 24 March 2025; accepted 7 April 2025. Date of publication 11 April 2025; date of current version 11 July 2025. This work was supported in part by the King Abdullah University of Science and Technology (KAUST) Office of Sponsored Research (OSR) under Award RFS-CRG12-2024-6478; in part by the European Commission through the Horizon Europe/JU SNS Project Hexa-X-II under Grant 101095759; in part by the Swedish Research Council VR under Grant 2023-03821 and Grant 2024-04390; and in part by the Chalmers Transport Area of Advance project “Towards a Multi-Layer Security Vision for Transportation Systems in the 6G Era”. The associate editor coordinating the review of this article and approving it for publication was Z. Becvar. (*Corresponding author: Hui Chen.*)

Yuchen Zhang and Tareq Y. Al-Naffouri are with the Electrical and Computer Engineering Program, Computer, Electrical and Mathematical Sciences and Engineering, King Abdullah University of Science and Technology, Thuwal 23955-6900, Saudi Arabia (e-mail: yuchen.zhang@kaust.edu.sa; tareq.alnaffouri@kaust.edu.sa).

Hui Chen, Musa Furkan Keskin, Alireza Pourafzal, and Henk Wymeersch are with the Department of Electrical Engineering, Chalmers University of Technology, 41296 Gothenburg, Sweden (e-mail: hui.chen@chalmers.se; furkan@chalmers.se; alireza.pourafzal@chalmers.se; henkw@chalmers.se).

Pinjun Zheng is with the School of Engineering, The University of British Columbia, Kelowna, BC V6T 1Z4, Canada (e-mail: pinjun.zheng@ubc.ca).

Digital Object Identifier 10.1109/LWC.2025.3560219

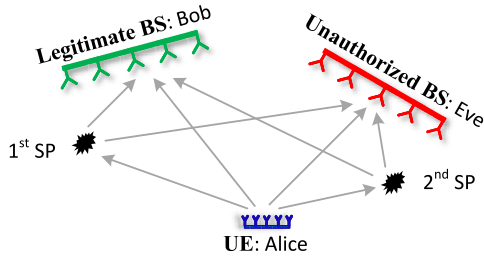


Fig. 1. Illustration of the risk of location privacy leakage in a MIMO OFDM localization system with coexisting legitimate and unauthorized nodes.

a novel beamforming technique that enhances legitimate localization performance while maintaining designated privacy levels. (iii) We demonstrate with numerical results the superior performance of the proposed beamforming approach compared to other benchmarks.

II. SYSTEM MODEL AND PROBLEM FORMULATION

As shown in Fig. 1, we consider a MIMO-OFDM-based uplink localization system with M subcarriers. Alice equipped with M_A transmit antennas, sends publicly known OFDM pilot signals over L time slots. Bob with M_B antennas, processes the received signals to estimate Alice's location. However, due to the inherent broadcast nature of wireless communication, Eve equipped with M_E antennas, can also intercept the signals and perform the same localization, leading to unwanted leakage of Alice's location information.

We assume that the locations of both Bob and Eve are known to Alice, as they typically have fixed locations as BSs. Additionally, the channels from Alice to Bob and from Alice to Eve are both influenced by the same group of scatter points (SPs). For the sake of conciseness, we use Bob's localization as an example and derive the performance based on the CRB. Due to the symmetry of the problem, the localization performance at Eve can be obtained directly.

A. Signal Model

Let N represent the number of OFDM pilot symbols per slot. The transmitted signal for the n -th symbol in the l -th slot over the m -th subcarrier is expressed as

$$\mathbf{x}[l, n, m] = \mathbf{w}[l]s[n, m], \quad (1)$$

where $\mathbf{w}[l] \in \mathbb{C}^{M_B}$ is the beamformer¹ in the l -th slot, and $s[n, m]$ is the unit-modulus pilot symbol on subcarrier m . The Alice-to-Bob channel for subcarrier m is modeled as

$$\mathbf{H}_B[m] = \sum_{k=0}^K \alpha_{B,k} e^{-j2\pi m \Delta f \tau_{B,k}} \mathbf{a}_B(\theta_{B,k}) \mathbf{a}_A^H(\theta_{A,k}), \quad (2)$$

where K denotes the number of SPs, while $\alpha_{B,k}$, $\tau_{B,k}$, $\theta_{B,k}$, and $\theta_{A,k}$ refer to the complex gain, delay, angle-of-arrival (AOA), and angle-of-departure (AOD) of the k -th SP, respectively. Note that for simplicity, the line-of-sight (LOS) path is indexed by $k = 0$. Here, $\theta_{B,0}$ and $\theta_{A,0}$ represent the AOA and AOD at Bob and Alice, respectively. Finally,

¹To reduce computational complexity, especially in practical systems with many subcarriers, we adopt the approach in [12], [13], where the beamformer maintains coherence across subcarriers, similar to analog beamforming, while still allowing amplitude and phase control. Although less flexible than conventional digital beamforming, it balances performance and efficiency.

$\mathbf{a}_A(\theta) \in \mathbb{C}^{M_A}$ and $\mathbf{a}_B(\theta) \in \mathbb{C}^{M_B}$ denote the steering vectors at Alice and Bob, respectively. The received signal at Bob² is

$$\mathbf{y}_B[l, n, m] = \mathbf{H}_B[m]\mathbf{x}[l, n, m] + \mathbf{z}_B[l, n, m], \quad (3)$$

where $\mathbf{z}_B[l, n, m] \sim \mathcal{CN}(\mathbf{0}, \sigma^2 \mathbf{I}_{M_B})$ is the additive white Gaussian noise (AWGN) at Bob's receiver. Here, $\sigma^2 = FN_0\Delta f$ is the noise power, where F , N_0 , and Δf represent the noise figure, single-sided power spectral density (PSD), and subcarrier spacing, respectively.

B. CRB-Based Performance Metric

The channel domain parameters relevant to Alice-Bob link are represented as $\boldsymbol{\xi}_B = [\boldsymbol{\Theta}_A^T, \boldsymbol{\Theta}_B^T, \boldsymbol{\tau}_B^T, \boldsymbol{\alpha}_{B,R}^T, \boldsymbol{\alpha}_{B,I}^T]^T \in \mathbb{R}^{(5K+5)}$. Here, $\boldsymbol{\Theta}_A = [\theta_{A,0}, \dots, \theta_{A,K}] \in \mathbb{R}^{(K+1)}$ denotes the angles of departure (AODs), while $\boldsymbol{\Theta}_B = [\theta_{B,0}, \dots, \theta_{B,K}] \in \mathbb{R}^{(K+1)}$ refers to the angles of arrival (AOAs). The delay measurements are encapsulated in $\boldsymbol{\tau}_B = [\tau_{B,0}, \dots, \tau_{B,K}] \in \mathbb{R}^{(K+1)}$, and the real and imaginary parts of the complex channel gains are captured in $\boldsymbol{\alpha}_{B,R} = [\Re\{\alpha_{B,0}\}, \dots, \Re\{\alpha_{B,K}\}] \in \mathbb{R}^{(K+1)}$ and $\boldsymbol{\alpha}_{B,I} = [\Im\{\alpha_{B,0}\}, \dots, \Im\{\alpha_{B,K}\}] \in \mathbb{R}^{(K+1)}$, respectively. Utilizing the Slepian-Bangs formula [12], the (i, j) -th element of the channel-domain Fisher information matrix (FIM) $\mathbf{F}_c(\boldsymbol{\xi}_B)$ can be expressed as

$$\begin{aligned} [\mathbf{F}_c(\boldsymbol{\xi}_B)]_{i,j} &= \frac{2}{\sigma^2} \sum_{l=1}^L \sum_{n=1}^N \sum_{m=1}^M \Re \left\{ \frac{\partial \boldsymbol{\mu}_B[l, n, m]^H}{\partial [\boldsymbol{\xi}_B]_i} \frac{\partial \boldsymbol{\mu}_B[l, n, m]}{\partial [\boldsymbol{\xi}_B]_j} \right\} \\ &= \frac{2N}{\sigma^2} \sum_{m=1}^M \Re \left\{ \text{tr} \left(\frac{\partial \mathbf{H}_B[m]}{\partial [\boldsymbol{\xi}_B]_j} \mathbf{W} \mathbf{W}^H \frac{\partial \mathbf{H}_B[m]^H}{\partial [\boldsymbol{\xi}_B]_i} \right) \right\}, \quad (4) \end{aligned}$$

where $\boldsymbol{\mu}_B[l, n, m] = \mathbf{H}_B[m]\mathbf{x}[l, n, m]$ denotes the noise-free observation from (3), and $\mathbf{W} = [\mathbf{w}_1, \dots, \mathbf{w}_L] \in \mathbb{C}^{M_B \times L}$ encompasses L beamformers.

Since we focus on the localization performance, the location-domain parameters are consolidated as $\boldsymbol{\eta}_B = [\mathbf{p}_A^T, \phi_B, \mathbf{p}_1^T, \dots, \mathbf{p}_K^T, \Delta t_B, \boldsymbol{\alpha}_{B,R}^T, \boldsymbol{\alpha}_{B,I}^T] \in \mathbb{R}^{(4K+6)}$, where $\mathbf{p}_A \in \mathbb{R}^2$ indicates Alice's position, and $\mathbf{p}_k \in \mathbb{R}^2$ denotes the location of the k -th scatterer. The variable ϕ_B represents Alice's relative orientation in Bob's local coordinate system, while Δt_B accounts for the clock bias, reflecting the timing mismatch between Alice and Bob. Notably, the nuisance parameters $\boldsymbol{\alpha}_{B,R}$ and $\boldsymbol{\alpha}_{B,I}$ derived from the channel-domain parameter $\boldsymbol{\xi}_B$ persist in the location-domain parameter $\boldsymbol{\eta}_B$, as they do not provide beneficial information for estimating position. The location-domain FIM, $\mathbf{F}_p(\boldsymbol{\eta}_B)$, is calculated from the channel-domain FIM as follows

$$\mathbf{F}_p(\boldsymbol{\eta}_B) = \mathbf{J}_B^T \mathbf{F}_c(\boldsymbol{\xi}_B) \mathbf{J}_B, \quad (5)$$

where $\mathbf{J}_B \in \mathbb{R}^{(5K+5) \times (4K+6)}$ represents the Jacobian matrix, with its (i, j) -th element defined as $[\mathbf{J}_B]_{i,j} = \partial [\boldsymbol{\xi}_B]_i / \partial [\boldsymbol{\eta}_B]_j$. The CRB is utilized to assess the localization precision w. r. t. \mathbf{p}_A at Bob, offering a lower limit on the total variances for estimating \mathbf{p}_A , expressed as follows

$$\text{CRB}_B(\mathbf{p}_A) = \text{tr} \left(\left[\mathbf{F}_p(\boldsymbol{\eta}_B)^{-1} \right]_{1:2,1:2} \right). \quad (6)$$

²Essentially, (3) applies to both digital and analog combining, utilizing a DFT codebook over $M_B \times L$ frames [12]. Without loss of generality, we omit the possible presence of an analog combiner for simplicity.

C. Problem Formulation

From (4), it is clear that the CRB for localization performance at Bob, i.e., $\text{CRB}_B(\mathbf{p}_A)$, depends on the design of \mathbf{W} , which can be optimized through appropriate beamformer configurations. At the same time, the CRB for localization performance at Eve, represented as $\text{CRB}_E(\mathbf{p}_A)$, also depends on \mathbf{W} . To preserve location privacy, it is essential to enhance legitimate localization performance while limiting the performance at the unauthorized node. Hence, we formulate an optimization problem about \mathbf{W} that seeks to minimize the legitimate CRB, ensuring that the CRB at the unauthorized node remains above a specified threshold,³ expressed as

$$\min_{\mathbf{W}} \text{CRB}_B(\mathbf{p}_A) \quad (7a)$$

$$\text{s.t.} \quad \text{CRB}_E(\mathbf{p}_A) \geq \gamma, \quad (7b)$$

$$\text{tr}(\mathbf{W} \mathbf{W}^H) \leq P/M, \quad (7c)$$

where γ is Eve's CRB threshold, determined by the practical requirement, and P denotes the power budget. We set the right side of (7c) to P/M , ensuring that the total transmit power across subcarriers equals P . Note that both $\text{CRB}_B(\mathbf{p}_A)$ and $\text{CRB}_E(\mathbf{p}_A)$ are non-convex and non-concave functions of \mathbf{W} , respectively, complicating solving (7).

III. PDD-BASED BEAMFORMING FOR LOCATION PRIVACY PRESERVATION

In this section, we propose a beamforming scheme to address the non-convexity and privacy constraints in problem (7). The scheme consists of a two-stage process: (i) problem reformulation via matrix lifting to reveal hidden structures, and (ii) a PDD optimization framework [14] to effectively handle the remaining non-convex constraints.

A. Problem Reformulation

Following [15], the matrices on the right-hand side of (6) can be reformulated as $[\mathbf{F}_p(\boldsymbol{\eta}_B)^{-1}]_{1:2,1:2} = [\mathbf{Q} - \mathbf{G}\mathbf{Z}^{-1}\mathbf{G}^T]^{-1}$, where $\mathbf{Q} = [\mathbf{F}_p(\boldsymbol{\eta}_B)]_{1:2,1:2}$, $\mathbf{G} = [\mathbf{F}_p(\boldsymbol{\eta}_B)]_{1:2,3:4K+6}$, and $\mathbf{Z} = [\mathbf{F}_p(\boldsymbol{\eta}_B)]_{3:4K+6,3:4K+6}$. Let $\mathbf{V} = \mathbf{W} \mathbf{W}^H$. From (4) and (5), it follows that the elements of \mathbf{Q} , \mathbf{G} , and \mathbf{Z} are linear with respect to \mathbf{V} . To facilitate reformulation, we introduce an auxiliary variable $\mathbf{U} \in \mathbb{R}^{2 \times 2}$ and apply the Schur complement property, transforming (7) into the following equivalent form

$$\min_{\mathbf{V}, \mathbf{U}} \text{tr}(\mathbf{U}^{-1}) \quad (8a)$$

$$\text{s.t.} \quad \begin{bmatrix} \mathbf{Q} - \mathbf{U} & \mathbf{G} \\ \mathbf{G}^T & \mathbf{Z} \end{bmatrix} \succeq \mathbf{0}, \quad \mathbf{U} \succeq \mathbf{0}, \quad (8b)$$

$$\text{CRB}_E(\mathbf{p}_A) \geq \gamma, \quad (8c)$$

$$\text{tr}(\mathbf{V}) \leq P/M, \quad (8d)$$

³Note that knowledge of channel parameters, such as AOAs, AODs, delays, and channel gains, is crucial for CRB calculation and can be obtained from external sources or from reciprocity-based estimation. For example, in a time-division duplexing system, Bob and Eve, as base stations, transmit downlink pilots for channel estimation. Using reciprocity, Alice estimates the Alice-Bob and Alice-Eve channel parameters. The impact of practical estimation errors can be mitigated using robust optimization techniques [12], [13], which quantify uncertainties and optimize performance. A detailed analysis of these aspects is beyond this letter's scope and left for future work.

Algorithm 1 PDD-Based Algorithm for Solving (9)

```

1: Initialize:  $\Theta = \mathbf{0}$ ,  $\rho$ ,  $\delta$ ,  $k = 1$ ;
2: repeat
3:   Optimize  $(\mathbf{V}, \mathbf{U}, \Phi)$  via BCD;
4:   if  $h(\mathbf{V}, \Phi) \leq \zeta[k]$  then
5:      $\Phi = \Phi + \rho(\mathbf{F}_p(\boldsymbol{\eta}_E)\Phi - \mathbf{I})$ ;
6:   else
7:      $\rho = \delta\rho$ ;
8:   end if
9:    $k = k + 1$ 
10: until  $h(\mathbf{V}, \Phi)$  is below a specified threshold.
11: Output:  $\mathbf{V}, \mathbf{U}, \Phi$ .

```

$$\text{rank}(\mathbf{V}) = L. \quad (8e)$$

However, due to the non-convex constraints in (8c) and (8e), solving (8) remains challenging.

B. PDD-Based Optimization Framework

Recall that $\text{CRB}_E(\mathbf{p}_A) = \text{tr}([\mathbf{F}_p(\boldsymbol{\eta}_E)^{-1}]_{1:2,1:2})$. By introducing the auxiliary variable $\Phi \in \mathbb{R}^{(5K+5) \times (5K+5)}$, while ignoring (8e), we can relax (8) into

$$\min_{\mathbf{V}, \mathbf{U}, \Phi} \text{tr}(\mathbf{U}^{-1}) \quad (9a)$$

$$\text{s.t.} \quad \Phi_{1,1} + \Phi_{2,2} \geq \gamma, \quad \Phi \succeq \mathbf{0}, \quad (9b)$$

$$\mathbf{F}_p(\boldsymbol{\eta}_E)\Phi = \mathbf{I}, \quad (9c)$$

$$(8b), (8d), \quad (9d)$$

where $\mathbf{F}_p(\boldsymbol{\eta}_E) \in \mathbb{R}^{(5K+5) \times (5K+5)}$ is the corresponding location-domain FIM from Alice to Eve, whose elements are also linear with \mathbf{V} , and \mathbf{I} denotes the identity matrix such that Φ serves as the inverse matrix of $\mathbf{F}_p(\boldsymbol{\eta}_E)$.

The primary challenge in solving (9) lies in the non-convex equality constraint (9c), which can be effectively addressed using the PDD framework. As described in [14], the standard PDD framework employs a double-loop structure, where the inner loop optimizes the augmented Lagrangian problem (ALP) of the original problem using a block coordinate descent (BCD) approach, while the outer loop updates the Lagrangian dual variables and penalty factors.

1) *Augmented Lagrangian Problem:* For the inner loop of the PDD framework, the ALP for (9) is given by

$$\min_{\mathbf{V}, \mathbf{U}, \Phi} \text{tr}(\mathbf{U}^{-1}) + \frac{\rho}{2} \left\| \mathbf{F}_p(\boldsymbol{\eta}_E)\Phi - \mathbf{I} + \frac{1}{\rho} \Theta \right\|_F^2 \quad (10a)$$

$$\text{s.t.} \quad (8b), (8d), (9b), \quad (10b)$$

where $\Theta \in \mathbb{R}^{(5K+5) \times (5K+5)}$ and ρ are the Lagrangian dual variable and penalty factor, respectively.

2) *Solving ALP With BCD:* It can be observed that, with fixed Θ and ρ , (10) remains non-convex due to the presence of the bilinear term $\mathbf{F}_p(\boldsymbol{\eta}_E)\Phi$, as $\mathbf{F}_p(\boldsymbol{\eta}_E)$ is linear with \mathbf{V} . However, by leveraging the technique of BCD, the augmented Lagrangian problem (10) can be solved by alternately solving the following two problems, i.e., (11) and (12), in an iterative manner until convergence.

- With fixed Φ , the convex semi-definite programming (SDP) subproblem w. r. t. (\mathbf{V}, \mathbf{U}) is given by

$$\min_{\mathbf{V}, \mathbf{U}} \text{tr}(\mathbf{U}^{-1}) + \frac{\rho}{2} \left\| \mathbf{F}_p(\boldsymbol{\eta}_E)\Phi - \mathbf{I} + \frac{1}{\rho} \Theta \right\|_F^2 \quad (11a)$$

$$\text{s.t.} \quad (8b), (8d). \quad (11b)$$

- With fixed (\mathbf{V}, \mathbf{U}) , the convex SDP subproblem w. r. t. Φ is given by

$$\min_{\Phi} \left\| \mathbf{F}_p(\eta_E)\Phi - \mathbf{I} + \frac{1}{\rho}\Theta \right\|_F^2 \quad (12a)$$

$$\text{s.t.} \quad (9b). \quad (12b)$$

Following the principle of PDD framework[14], to ensure convergence, we define the violation function as $h(\mathbf{V}, \Phi) = \|\mathbf{F}_p(\eta_E)\Phi - \mathbf{I}\|_\infty$. The steps of (9) using the PDD approach is summarized in Algorithm 1. Here, $\delta > 1$ is a constant that increases the penalty factor when necessary, while $\zeta[k]$ denotes a sequence determined empirically to approach zero. Specifically, we define $\zeta[k] = qh^{(k-1)}(\mathbf{V}, \Phi)$, where $q \in (0, 1)$ is an attenuation constant, and $h^{(k-1)}(\mathbf{V}, \Phi)$ is the value of $h(\mathbf{V}, \Phi)$ at the $(k-1)$ -th iteration. After obtaining \mathbf{V} from Algorithm 1, the beamformers \mathbf{W} can then be derived from \mathbf{V} via matrix decomposition or randomization techniques [16].

C. Convergence and Complexity

As ρ increases, the term $\|\mathbf{F}_p(\eta_E)\Phi - \mathbf{I} + \frac{1}{\rho}\Theta\|_F$ tends to zero, indicating that the constraint (9c) in (9) is satisfied over iterations. A detailed discussion on the convergence of the PDD framework is provided in [14], which ensures the convergence of Algorithm 1.

The overall complexity of Algorithm 1 is primarily dictated by the inner BCD process. According to [12], the complexity of an SDP problem is $\mathcal{O}(I^2 \sum_{j=1}^J d_j^2 + I \sum_{j=1}^J d_j^3)$, where I and J denote the number of variables and linear matrix inequality (LMI) constraints, and d_j represents the size of the j -th matrix. For subproblem (11), the complexity is approximated as $\mathcal{O}(M_A^4 K^2 + M_A^2 K^3)$, and for subproblem (12), it is $\mathcal{O}(K^6)$.

IV. NUMERICAL RESULTS

A. Scenarios

The simulation setup assumes the following parameters unless otherwise specified: Alice is equipped with $M_A = 16$ transmit antennas and is located at $\mathbf{p}_A = [0\text{m}, 0\text{m}]^T$. Bob, also using $M_B = 16$ antennas, is placed at $\mathbf{p}_B = [-5\text{m}, 20\text{m}]^T$, while Eve, equipped with $M_E = 16$ antennas, is localized at $\mathbf{p}_E = [4\text{m}, 20\text{m}]^T$. Two SPs are present at $\mathbf{p}_1 = [-10\text{m}, 15\text{m}]^T$ and $\mathbf{p}_2 = [5\text{m}, 15\text{m}]^T$. The system's transmit power is $P = -20\text{dBm}$, with a carrier frequency of $f_c = 28\text{GHz}$ and a bandwidth of $W = 120\text{MHz}$. The number of subcarriers is $M = 1024$, the noise figure is $F = 10\text{dB}$, and the noise power spectral density is $N_0 = -173.855\text{dBm/Hz}$. The simulation covers $L = 16$ time slots, each containing $N = 100$ pilot OFDM signals. Bob's clock bias is $\Delta t_B = 1 \mu\text{s}$, and his relative orientation is $\phi_B = (110/180)\pi$, while Eve's clock bias and orientation are $\Delta t_E = 1 \mu\text{s}$ and $\phi_E = (200/180)\pi$, respectively. Channel gains follow a free-space path loss model[2]. For the Alice-Bob link, the LOS channel gain is $\alpha_{B,0} = e^{j\omega_{B,0}} \lambda / (4\pi \|\mathbf{p}_A - \mathbf{p}_B\|)$, and the non-line-of-sight (NLOS) gain is $\alpha_{B,k} = \sigma_{\text{RCS}} e^{j\omega_{B,k}} \lambda / ((4\pi)^{3/2} \|\mathbf{p}_A - \mathbf{p}_k\| \|\mathbf{p}_k - \mathbf{p}_B\|)$. Similarly, the LOS gain for the Alice-Eve link is $\alpha_{E,0} = e^{j\omega_{E,0}} \lambda / (4\pi \|\mathbf{p}_A - \mathbf{p}_E\|)$, and the NLOS gain is $\alpha_{E,k} = \sigma_{\text{RCS}} e^{j\omega_{E,k}} \lambda / ((4\pi)^{3/2} \|\mathbf{p}_A - \mathbf{p}_k\| \|\mathbf{p}_k - \mathbf{p}_E\|)$. Here, $\omega_{B,k}$ and $\omega_{E,k}$ are the uniformly distributed random

phases of Alice-Bob and Alice-Eve links, respectively. The radar cross section (RCS) for each SP is $\sigma_{\text{RCS}} = 100\text{m}^2$, and the wavelength is $\lambda = c/f_c$, where c represents the speed of light.

B. Benchmarks

For comparison, we introduce two power-adjustment-based benchmarks, which are detailed below:

- *Benchmark I:* By ignoring the location privacy constraint (7b), (7) reduces to a location-domain CRB minimization problem, which can be solved using the approach proposed in [12]. If the solution already satisfies (7b), we retain the obtained beamformers. Otherwise, we reduce the transmit power until (7b) holds with equality.
- *Benchmark II:* We first obtain beamformers using the low-complexity, codebook-based power allocation scheme from [12], [13], which exploits the structure of the optimal variance matrix to minimize the CRB. As in Benchmark I, we then adjust the transmit power based on the same principle.

C. Results and Discussion

1) *Beam patterns:* Figures 2(a)-(d) illustrate the beam patterns (normalized receive powers) of the proposed beamforming approach for different values of γ , representing varying levels of location privacy requirements. When $\sqrt{\gamma} = 0\text{m}$, meaning no location privacy constraint is applied, the problem reduces to the CRB-minimizing problem addressed in [12]. As shown in Fig. 2(a), Bob, serving as the sole anchor with a known position, and two SPs, which create resolvable paths advantageous for single-anchor localization, are simultaneously illuminated by three beams. As γ increases, implying a stricter location privacy constraint, the beam illuminating the SP on the right, which is closer to Eve, diminishes. This occurs because energy leakage to Eve must be minimized, thereby protecting Alice's location privacy at the cost of Bob's localization performance. As γ increases further, such as when $\sqrt{\gamma}$ reaches 10m , even the beam on the left slightly shifts away from the illuminated SP, which could otherwise enhance Eve's localization performance.

2) *Comparison Between Different Schemes:* Figures 3(a) and (b) compare the proposed beamforming approach with benchmark methods, evaluating Bob's localization performance (characterized by the CRB) and the allowable transmit power against the requirement for location privacy protection (characterized by $\sqrt{\gamma}$), respectively. From Fig. 3(a), we observe that the proposed scheme significantly outperforms the two benchmarks in achieving lower CRB for a given γ . Notably, when $\sqrt{\gamma} = 0\text{m}$, Bob's CRB under the proposed scheme equals that under Benchmark I, as they are equivalent at this point. In contrast, Benchmark II results in a slightly higher CRB, as it reduces complexity at the cost of degraded localization performance [12]. As shown in Fig. 3(b), the superiority of the proposed scheme arises from its ability to maintain full transmit power, while the benchmarks must reduce transmit power to satisfy the location privacy constraint (except when γ is very small, where the privacy constraints are not restricted). This advantage is due to the proposed scheme's ability to manage energy leakage to Eve by judiciously

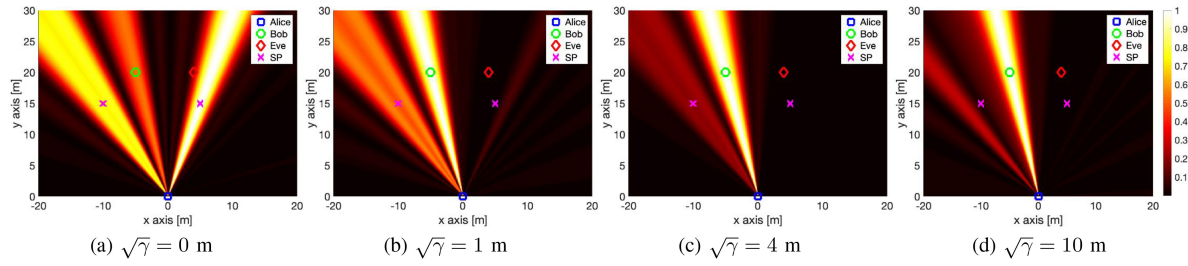


Fig. 2. Beam patterns under different location privacy constraint: (a) $\sqrt{\gamma} = 0$ m; (b) $\sqrt{\gamma} = 1$ m; (c) $\sqrt{\gamma} = 4$ m; (d) $\sqrt{\gamma} = 10$ m.

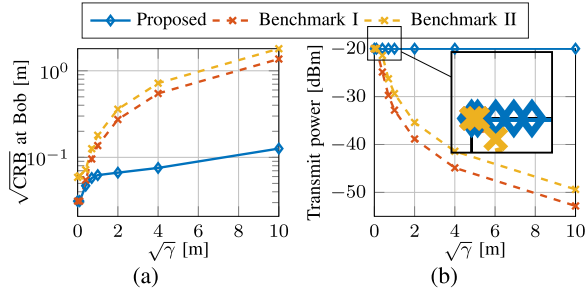


Fig. 3. Comparison between the proposed scheme and benchmarks: (a) $\sqrt{\text{CRB}}$ at Bob versus $\sqrt{\gamma}$; (b) Allowable transmit power versus $\sqrt{\gamma}$.

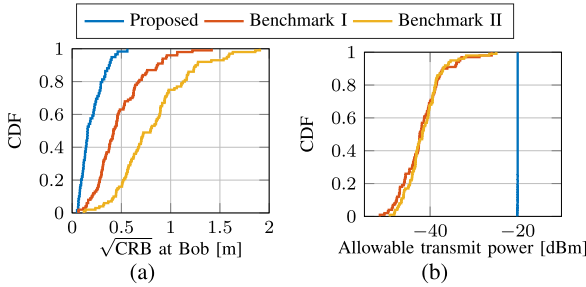


Fig. 4. Comparison between the proposed scheme and benchmarks: (a) CDF of $\sqrt{\text{CRB}}$ at Bob; (b) CDF of allowable transmit power.

exploiting spatial degrees of freedom, allowing the location privacy constraint to be met without compromising transmit power, in sharp contrast to the benchmarks.

Figures 4(a) and (b) compare the cumulative distribution functions (CDFs) of the CRBs at Bob and the allowable transmit power at Alice, respectively, where Bob, Eve, and SPs are randomly distributed within $5\text{m} \times 5\text{m}$ areas centered at the locations specified in Section IV-A, with $\sqrt{\gamma} = 5\text{m}$. As observed, the proposed approach achieves a significantly lower range of CRB values and higher range of transmit power compared to Benchmarks I and II, aligning with the observations in Fig. 3 and further validating its superiority in a broader sense.

V. CONCLUSION

We examine a localization scenario involving uplink MIMO-OFDM where a legitimate BS sought to determine the location of a UE, while an unauthorized BS jeopardizes the UE's privacy by eavesdropping on pilot signals to estimate its position. To improve legitimate localization while safeguarding privacy, we formulate an optimization problem aimed at minimizing the CRB for legitimate localization, subject to constraints on unauthorized localization. Leveraging a PDD framework, we propose an innovative beamforming strategy.

Numerical simulations validate our approach's effectiveness, showcasing its advantages over established benchmarks.

While this letter focuses on a 2D scenario, the methodology can be extended to a 3D scenario, which introduces higher complexity and is left for future research. Additionally, employing a reconfigurable intelligent surface, which serves as a controllable SP with the ability to cooperate with the BS, to further enhance privacy warrants further study.

REFERENCES

- [1] L. Italiano et al., "A tutorial on 5G positioning," *IEEE Commun. Surveys Tuts.*, early access, Aug. 23, 2024, doi: [10.1109/COMST.2024.3449031](https://doi.org/10.1109/COMST.2024.3449031).
- [2] H. Wymeersch and G. Seco-Granados, "Radio localization and sensing—Part I: Fundamentals," *IEEE Commun. Lett.*, vol. 26, no. 12, pp. 2816–2820, Dec. 2022.
- [3] X. Chen et al., "A survey on multiple-antenna techniques for physical layer security," *IEEE Commun. Surveys Tuts.*, vol. 19, no. 2, pp. 1027–1053, 2nd Quart., 2017.
- [4] R. Chen et al., "Reconfigurable intelligent surfaces for 6G IoT wireless positioning: A contemporary survey," *IEEE Internet Things J.*, vol. 9, no. 23, pp. 23570–23582, Dec. 2022.
- [5] S. Roth et al., "Localization attack by precoder feedback overhearing in 5G networks and countermeasures," *IEEE Trans. Wireless Commun.*, vol. 20, no. 7, pp. 4100–4112, Jul. 2021.
- [6] J. Li and U. Mitra, "Channel state information-free location-privacy enhancement: Fake path injection," *IEEE Trans. Signal Process.*, vol. 72, pp. 3745–3760, Aug. 2024.
- [7] Y. Zhang et al., "Privacy preservation in delay-based Localization systems: Artificial noise or artificial multipath?" in *Proc. IEEE Glob. Commun. Conf. (GLOBECOM)*, 2024, pp. 2755–2760.
- [8] P. Huang et al., "Attacking and defending deep-learning-based off-device wireless positioning systems," *IEEE Trans. Wireless Commun.*, vol. 23, no. 8, pp. 8883–8895, Aug. 2024.
- [9] Y. Zhang et al., "Near-field wideband secure communications: An analog beamfocusing approach," *IEEE Trans. Signal Process.*, vol. 72, pp. 2173–2187, Apr. 2024.
- [10] J. J. Checa and S. Tomasin, "Location-privacy-preserving technique for 5G mmWave devices," *IEEE Commun. Lett.*, vol. 24, no. 12, pp. 2692–2695, Dec. 2020.
- [11] S. Tomasin, "Beamforming and artificial noise for cross-layer location privacy of E-health cellular devices," in *Proc. IEEE Int. Conf. Commun. Workshops (ICC Workshops)*, 2022, pp. 568–573.
- [12] M. F. Keskin et al., "Optimal spatial signal design for mmWave positioning under imperfect synchronization," *IEEE Trans. Veh. Technol.*, vol. 71, no. 5, pp. 5558–5563, May 2022.
- [13] A. Fascista et al., "RIS-aided joint localization and synchronization with a single-antenna receiver: Beamforming design and low-complexity estimation," *IEEE J. Sel. Topics Signal Process.*, vol. 16, no. 5, pp. 1141–1156, Aug. 2022.
- [14] Q. Shi and M. Hong, "Penalty dual decomposition method for nonsmooth nonconvex optimization—Part I: Algorithms and convergence analysis," *IEEE Trans. Signal Process.*, vol. 68, pp. 4108–4122, Jun. 2020.
- [15] R. Mendrzik et al., "Harnessing NLOS components for position and orientation estimation in 5G millimeter wave MIMO," *IEEE Trans. Wireless Commun.*, vol. 18, no. 1, pp. 93–107, Jan. 2019.
- [16] Z.-Q. Luo et al., "Semidefinite relaxation of quadratic optimization problems," *IEEE Signal Process. Mag.*, vol. 27, no. 3, pp. 20–34, May 2010.